Structure-kinetic relationship studies of cannabinoid CB_2 receptor agonists reveal substituent-specific lipophilic effects on residence time

Marjolein Soethoudt, Mark W.H. Hoorens, Ward Doelman, Andrea Martella, Mario van der Stelt, Laura H. Heitman

PII: S0006-2952(18)30123-0
DOI: https://doi.org/10.1016/j.bcp.2018.03.018
Reference: BCP 13095

To appear in: *Biochemical Pharmacology*

Received Date: 9 January 2018
Accepted Date: 16 March 2018

Please cite this article as: M. Soethoudt, M.W.H. Hoorens, W. Doelman, A. Martella, M. van der Stelt, L.H. Heitman, Structure-kinetic relationship studies of cannabinoid CB_2 receptor agonists reveal substituent-specific lipophilic effects on residence time, *Biochemical Pharmacology* (2018), doi: https://doi.org/10.1016/j.bcp.2018.03.018

Structure-kinetic relationship studies of cannabinoid CB_2 receptor agonists reveal substituent-specific lipophilic effects on residence time

Marjolein Soethoudt,[1,2] Mark W.H. Hoorens,[2] Ward Doelman,[2] Andrea Martella,[2] Mario van der Stelt,[2] Laura H. Heitman[1]

[1]Division of Drug Discovery and Safety, Leiden Academic Centre for Drug Research, University of Leiden, Einsteinweg 55, 2333 AR, The Netherlands

[2]Department of Molecular Physiology, Leiden Institute of Chemistry, University of Leiden, Einsteinweg 55, 2333 AR, The Netherlands

Author for correspondence: Laura H. Heitman, Tel.: +31 71 5274558, l.h.heitman@lacdr.leidenuniv.nl

Key words: Target residence time, Physicochemical properties, Cannabinoid CB_2 receptor, Functional potency

Abstract

A decade ago, the drug-target residence time model has been (re-)introduced, which describes the importance of binding kinetics of ligands on their protein targets. Since then, it has been applied successfully for multiple protein targets, including GPCRs, for the development of lead compounds with slow dissociation kinetics (i.e. long target residence time) to increase *in vivo* efficacy or with short residence time to prevent on-target associated side effects. To date, this model has not been applied in the design and pharmacological evaluation of novel selective ligands for the cannabinoid CB_2 receptor (CB_2R), a GPCR with therapeutic potential in the treatment of tissue injury and inflammatory diseases. Here, we have investigated the relationships between physicochemical properties, binding kinetics and functional activity in two different signal transduction pathways, G protein activation and β-arrestin recruitment. We synthesized 24 analogues of 3-cyclopropyl-1-(4-(6-((1,1-dioxidothiomorpholino)methyl)-5-fluoropyridin-2-yl)benzyl)imidazoleidine-2,4-dione (LEI101), our previously reported *in vivo* active and CB_2R-selective agonist, with varying basicity and lipophilicity. We identified a positive correlation between target residence time and functional potency due to an increase in lipophilicity on the alkyl substituents, which was not the case for the amine substituents. Basicity of the agonists did not show a relationship with affinity, residence time or functional activity. Our findings provide important insights about the effects of physicochemical properties of the specific substituents of this scaffold on the binding kinetics of agonists and their CB_2R pharmacology. This work therefore shows how CB_2R agonists can be designed to have optimal kinetic profiles, which could aid the lead optimization process in drug discovery for the study or treatment of inflammatory diseases.

1. Introduction

Traditionally, in drug discovery, the affinity or potency of a drug candidate for a given target was considered a key determinant for *in vivo* activity, but later it was found that these parameters do not correlate as well as originally thought.[1, 2] In contrast, the binding kinetics of a ligand for a given target, in particular slow dissociation kinetics and therefore a long target residence time, may be a better predictor of *in vivo* efficacy in specific cases,[3-6] as emphasized by several excellent reviews.[7-9] For example, a correlation was found between long residence time of Fab-I enoyl reductase inhibitors and their *in vivo* activity in a mouse model of tularemia infection, leading to prolonged survival of the mice.[3, 4] Recently, this "drug-target residence time model" has aided several clinical-stage drug development programs[10, 11] by selecting compounds with high efficacy,[12] or reduced on-target toxicities.[13] However, the association rate is increasingly recognized as well as an important factor in determining a ligand's functional activity. For example, slowly associating ligands may decrease on-target related side effects by preventing high target occupancy and fast target activation,[14] while fast associating ligands may have an influence in prolonged activity if rebinding occurs.[15]

Retrospective analysis of marketed drugs for G protein-coupled receptors (GPCRs), an important class of drug targets, revealed that the beneficial effects of some of these drugs may be attributed to their long drug-target residence times.[8] Interestingly, in case of GPCR agonists, a positive correlation was also found between long residence time and *in vitro* efficacy for the Adenosine A_{2A} receptor[16] and the Muscarinic M_3 receptor.[17] For the latter, it was also shown that long target residence time of an antagonist, i.e. tiotropium, resulted in so-called kinetic selectivity

over the other muscarinic receptor subtypes, thereby reducing off-target side effects.[18]

The cannabinoid CB_1 and CB_2 receptor (CB_1R and CB_2R) are class A GPCRs and both part of the endocannabinoid system. This signaling system comprises the receptors as well as their endogenous ligands, anandamide (AEA) and 2-arachidoylglycerol (2-AG), which are called endocannabinoids.[19] The CB_1R is mainly found within the central nervous system,[20] which is therefore mainly responsible for the psycho-active effects of Δ^9-tetrahydrocannabinol (THC), the main active substituent in cannabis.[21] In contrast, the CB_2R is predominantly abundant in immune cells, is involved in cell migration and immunosuppression,[22, 23] and is upregulated during pathophysiological conditions.[24] CB_2R activity has been associated with therapeutic benefits in inflammatory or immune system related pathologies.[24, 25] Selective activation of the CB_2R is therefore associated with therapeutic benefits and may prevent CB_1R-mediated adverse side effects.

Recently, our group reported on 3-cyclopropyl-1-(4-(6-((1,1-dioxidothiomorpholino)methyl)-5-fluoropyridin-2-yl)benzyl)imidazoleidine-2,4-dione (LEI101) (**Figure 1**), a promising CB_2R partial agonist.[26] LEI101 showed *in vivo* efficacy in preclinical models of neuropathic pain and *cis*-platin-induced nephrotoxicity.[26],[27] The CB_2R kinetic profile of LEI101 is unknown, therefore we were interested to systematically investigate the binding kinetics and functional activity of this chemical series.

To this end, we synthesized a library of 24 compounds based on the scaffold of LEI101 (**Figure 1**), in which we systematically varied their basicity and lipophilicity (pK_a and LogP) of the R^1 (amine) and R^2 (alkyl) substituents and determined their equilibrium binding affinity and Kinetic Rate Index (KRI), a high-throughput measure

as an indication for ligand-receptor kinetics.[28] In addition, the full kinetic profile, as well as functional potency and efficacy in G protein activation and β-arrestin recruitment, was measured for 14 of these compounds. Correlation analysis of the data identified a relationship between target residence time and potency in both signal transduction pathways due to increased lipophilicity specifically on the R^2 position. This work provides important insights in the impact of divergent binding kinetics of LEI101-based agonists on CB_2R pharmacology and the role of physicochemical properties therein. In turn, these insights show how CB_2R agonists can be designed to have optimal kinetic profiles, which will aid the lead optimization process in drug discovery for the study or treatment of inflammatory diseases.

2. Materials and Methods

2.1 Chemical and reagents

All common reagents were purchased from commercial sources and used as received. The agonist library was synthesized as described previously in van der Stelt *et al,* 2011,[27] with only small modifications (see **Figure 2**). After purification, all compounds had more than 95% purity as determined by Liquid Chromatography Mass Spectroscopy (LCMS), by measuring UV absorbance at 254 nm and were fully characterized using ^{1}H-NMR and ^{13}C-NMR. High resolution mass spectra were recorded on a mass spectrometer (Thermo Finnigan LTQ Orbitrap) equipped with an electrospray ion source (ESI) in positive mode. The spectrometer was calibrated prior to each measurement with a calibration mixture (Thermo Finnigan). Molecules are drawn with ChemDraw Professional 16.0. Full details regarding synthetic procedures and compound characterization can be provided upon request from the corresponding author. Cell culture medium components (Ham's F12 Nutrient Mixture, gllutamine and antibiotics penicillin, streptomycin, hygromycin and geneticin), bovine serum albumin (BSA), polyethylenedimide (PEI), guanosine diphosphate (GDP), dithiothreitol (DTT) and cannabinoid receptor ligands CP55940 and AM630 were purchased from Sigma Aldrich (St. Louis, MO). [^{3}H]CP55940 (specific activity 141.2 Ci/mmol), [^{35}S]GTPγS (specific activity 1250 Ci/mmol) and GF-B/GF-C filters were purchased from Perkin Elmer (Waltham, MA). Bicinchoninic acid (BCA) and BCA

protein assay reagent were obtained from Pierce Chemical Company (Rochford, IL). The PathHunter® CHO-K1 CNR1 (CHOK1hCB$_1$_bgal) and CNR2 (CHOK1hCB$_2$_bgal) β-Arrestin Cell Lines and the PathHunter® detection kit were obtained from DiscoveRx (Fremont, United States). Cell culture plates were purchased from Sarstedt and 384-well white walled assay plates from Perkin Elmer. All buffers and solutions were prepared using Millipore water (deionized using a MilliQ A10 Biocel^{TM}, with a 0.22 µm filter) and analytical grade reagents and solvents. Buffers are prepared at room temperature and stored at 4°C, unless stated otherwise.

2.2 Cell culture

CHOK1hCB$_2$_bgal cells were cultured in Ham's F12 Nutrient Mixture, supplemented with 10% fetal calf serum, 1 mM glutamine, 50 U/mL penicillin, 50 µg/mL streptomycin, 300 mg/mL hygromycin and 800 µg/mL geneticin in a humidified atmosphere at 37°C and 5% CO_2, as reported previously.[29] Cells were subcultured twice a week at a ratio of 1:20 on 10-cm diameter plates by trypsinization. For membrane preparation the cells were subcultured 1:10 and transferred to 15-cm diameter plates. Cells were passaged no longer than 25 times or 3 months.

2.3 Membrane preparation

Per batch of membranes, cells on thirty 15-cm ø plates were detached from the bottom by scraping them into 5 mL phosphate-buffered saline (PBS), collected in 12 mL Falcon tubes and centrifuged for 5 minutes at 200 g (3,000 rpm). The pellets were resuspended in ice-cold 50 mM Tris-HCl buffer and 5 mM $MgCl_2$ (pH 7.4). An Ultra Thurrax homogenizer (Heidolph Instruments, Schwabach, Germany) was used to homogenize the cell suspension. The membranes and cytosolic fractions were separated by centrifugation at 100,000 g (31,000 rpm) in a Beckman Optima LE-80 K ultracentrifuge (Beckman Coulter Inc., Fullerton, CA) at 4°C for 20 minutes. The pellet was resuspended in 10 mL of Tris-HCl buffer and 5 mM $MgCl_2$ (pH 7.4) and the homogenization and centrifugation steps were repeated. Finally, the membrane pellet was resuspended in 10 mL 50 mM Tris-HCl buffer and 5 mM $MgCl_2$ (pH 7.4) and aliquots of 250 µL were stored at -80°C. Membrane protein concentrations were measured using the BCA method.[30]

2.4 [^{3}H]CP55940 equilibrium displacement assay

[^{3}H]CP55940 displacement assays were used for the determination of affinity (IC_{50}) values of unlabeled ligands. Membrane aliquots containing 1.5 µg of membrane protein were incubated in a total volume of 100 µL assay buffer (50 mM Tris-HCl buffer (pH 7.4), 5 mM $MgCl_2$ and 0.1% BSA) at 25°C for 2 hours in presence of ~1.5 nM [^{3}H]CP55940. Ten different concentrations of competing ligand were used for determination of IC_{50} values, and nonspecific binding was determined in the presence of 10 µM AM630. Incubations were terminated and samples harvested as described by the **96-wells harvest procedure** (see below).

2.5 96-wells harvest procedure

Samples were harvested on 96-wells GF/C filters, precoated with 25 µL 0.25% (v/v) PEI per well, with rapid vacuum filtration, to separate the bound and free radioligand, using a Perkin Elmer 96-wells harvester (Perkin Elmer, Groningen, The Netherlands). Filters were subsequently washed ten times with ice-cold assay buffer on the 96-well plate and 5 times on a wash plate. Filter plates were dried at 55°C for ~45 min, then 25 µL Microscint was added per well (Perkin Elmer, Groningen, The Netherlands). After 3 hours, the filter-bound radioactivity was determined by scintillation spectrometry using a Microbeta2® 2450 microplate counter (Perkin Elmer, Boston, MA).

2.6 [^{3}H]CP55940 Association Assay

To determine association kinetics of [^{3}H]CP55940, it was incubated at a concentration of ~1.5 nM with 1.5 µg of membrane protein in a total volume of 100 µL of assay buffer at 25°C or 10°C for a range of timepoints (90, 60, 30, 25, 20, 15, 10, 5, 3 and 1 minutes). For the assay at 10°C, an additional time point at 120 min was added. Nonspecific binding was determined in the presence of 10 µM AM630. Incubations were terminated and samples harvested as described by the **96-wells harvest procedure** (see above).

2.7 [^{3}H]CP55940 Dissociation Assay

To determine dissociation kinetics of [^{3}H]CP55940, it was incubated at a concentration of ~1.5 nM with 1.5 µg of membrane protein in a total volume of 100 µL of assay buffer at 25°C or 10°C for 2 hr. Dissociation was then initiated at a range of timepoints (25°C: 90, 30, 20, 15, 10, 8, 5, 3, 1 min; 10°C:

360, 300, 240, 180, 120, 90, 60, 30, 10 and 5 min) by addition of 5 µL of AM630 (final assay concentration: 10 µM). Nonspecific binding was determined by addition of 10 µM AM630 from the start of the assay. Incubations were terminated and samples harvested as described by the **96-wells harvest procedure** (see above).

2.8 [^{3}H]CP55940 Dual-point Competition Association Assay

For fast determination of the relative kinetics of the agonist library, the KRI was determined using a dual-point competition association assay.[13] The agonists were incubated at their IC_{50} concentration (as determined at 25°C) with 1.5 nM of [^{3}H]CP55940 and 1.5 µg membrane protein in assay buffer in a total volume of 100 µL, for either 1 or 2 hours at 10°C (t_1 and t_2, respectively). Nonspecific binding was determined by addition of 10 µM AM630 from the start of the assay. Incubations were terminated and samples harvested as described by the **96-wells harvest procedure** (see above).

2.9 [^{3}H]CP55940 Full Competition Association Assay

To determine the k_{on} and k_{off} values of unlabeled competing ligands. Ligands were incubated at their IC_{50} concentration (see **2.12 Data Analysis**) in presence of ~1.5 nM [^{3}H]CP55940 and with 1.5 µg of membrane protein in a total volume of 100 µL of assay buffer at 10 °C for a range of timepoints (120, 90, 60, 30, 25, 20, 15, 10, 5, 3 and 1 minutes). Nonspecific binding was determined in the presence of 10 µM AM630. Incubations were terminated and samples harvested as described by the **96-wells harvest procedure** (see above).

2.10 [^{35}S]GTPγS assay

G protein activation as a measure for receptor activity was determined by the binding of radiolabeled non-hydrolyzable GTP ([S^{35}]GTPγS) to the receptor.[29, 31] To homogenized CHOK1CB_2R_bgal membranes (5 µg) in 20 µL assay buffer (50 mM Tris-HCl buffer (pH 7.4), 5 mM $MgCl_2$, 150 mM NaCl, 1 mM EDTA, 0.05% BSA and 1 mM DTT, freshly prepared every day), 5 µg saponin and 1 µM GDP were added (final assay concentration). To determine the pEC_{50} and E_{max} values of the agonist library, the membranes were directly incubated for 30 min at room temperature with various concentrations of the ligands of interest. The basal level of [S^{35}]GTPγS binding was measured in untreated membrane samples, and the maximal level of [S^{35}]GTPγS binding was measured by treatment of the membranes

with 10 µM CP55940. Subsequently, [$S^{35}S$]GTPγS (0.3 nM) was added and the samples were incubated for 90 minutes at 25 °C on a shaking platform in a total sample volume of 100 µL. Incubations were terminated and samples harvested as described by the **96-wells harvest procedure** (see above). Here, samples were harvested on 96-wells GF/B filters and washed using buffer containing 50 mM Tris HCl, pH 7.4 and 5 mM $MgCl_2$.

2.11 PathHunter® β-Arrestin Recruitment Assay

The assay was performed using the PathHunter® CHOK1CB_2R_bgal cells and β-arrestin recruitment assay kit (DiscoveRx Corporation, Fremont, CA), as published before.[29, 32] Briefly, PathHunter® CHOK1hCB_2R_bgal cells were seeded at a density of 5000 cells per well of solid white walled 384-well plates (Perkin Elmer, MA, USA) in 20 µL HAM's F12 Nutrient Mixture culture medium and incubated overnight in a humidified atmosphere at 37°C and 5% CO_2. The cells were stimulated with 5 µL of 50 µM (10 µM final assay concentration) of each agonist (single point assay) or 10 increasing concentrations of each agonist and incubated for 90 minutes in a humidified atmosphere at 37°C and 5% CO_2. The DMSO concentration was the same in each well. The activity of β-galactosidase was determined using the PathHunter® Detection Kit (DiscoveRx Corporation, Fremont, CA), following the supplier's protocol. In short, the cells were loaded with 12 µL detection reagent (DiscoveRx Corporation, Fremont, CA) and incubated for 1 hour in the dark at room temperature. Luminescence (400-700 nm), indicated as relative light units (RLU), was measured on an EnVision multilabel plate reader (Perkin Elmer, MA, USA), using a Luminescence 700 emission filter.

2.12 Data Analysis

cLogP and pK_a values were calculated using ChemDraw® Professional 16.0 (Perkin Elmer). All experimental data were analyzed using the nonlinear regression curve fitting program GraphPad Prism 7 (GraphPad Software, Inc., San Diego, CA). From displacement assays at 25°C, the non-linear regression analysis for one site - Fit Ki was used to obtain $logK_i$ values, which are provided by Prism by direct application of the Cheng-Prusoff equation:[33] $K_i = IC_{50} / (1 + ([L]/K_D))$ in which [L] is the exact concentration of [^{3}H]CP55940 determined per experiment (i.e. ~1.5 nM). The kinetic K_D (1.24 ± 0.10 nM) of [^{3}H]CP55940 was calculated using the formula $K_D = k_{off}/k_{on}$. The k_{on} (1.6 ± 0.1 x 10^6 M^{-1} s^{-1}) and k_{off} (2.0 ± 0.1 x 10^{-3} s^{-1}) of [^{3}H]CP55940 at this temperature were determined using an

association and dissociation assay, respectively (three experiments performed in duplicate, data not shown). The $logK_i$ values were converted manually to pK_i values (**Table 1**). For the kinetic experiments, a concentration equal to the IC_{50} value of each agonist was used, as determined from the non-linear regression analysis for "one site - Fit $logIC_{50}$". For non-linear regression analysis "one site - Fit K_i" and "one site - Fit $logIC_{50}$" the top and bottom of the curve were constrained at 100 and 0, respectively. From association assays, the association rate constant (k_{on}) of [^{3}H]CP55940 was calculated using the formula $k_{on}=(k_{obs}-k_{off})/[L]$, in which [L] is the exact concentration of [^{3}H]CP55940 determined per experiment. The observed association rate (k_{obs}) was determined with Prism's "one-phase exponential association" analysis that uses the following formula: $Y = Y0 + (Plateau – Y0) * (1 – exp(-k_{obs}* t)$, where Y0 is the specific radioligand binding at time 0 (constrained at 0), Plateau represents the maximum specific [^{3}H]CP55940 binding at equilibrium, k_{obs} is the observed association rate in min^{-1} and t is the time in minutes. From dissociation assays, the dissociation rate constant (k_{off}) of [^{3}H]CP55940 was determined using Prism's "one-phase exponential decay" analysis using the following formula: $Y = (Y0 – NSB) * exp(-k_{off} * t) + NSB$, where k_{off} is the dissociation rate constant in min^{-1} and where Y0 is the specific radioligand binding at time 0 (constrained at 100). From competition association assays, the k_{on} and the k_{off} of cold ligands were obtained by non-linear regression analysis "kinetics of competitive binding" that uses the following equation:[34]

$[RL] = Q*((k_4DIFF)/(K_FK_S)) + ((k_4 – K_F)/K_F)*exp(-K_Ft) – ((k_4 – K_S)/K_S)*exp(-K_St)$, using the following variables:

$K_A = k_1[L](10^{-9}) + k_2$

$K_B = k_3[I](10^{-9}) + k_4$

$S = \sqrt{((K_A – K_B)^2 + 4*k_1k_3[L][I](10^{-18}))}$

$K_F = 0.5 * (K_A + K_B + S)$

$K_S = 0.5 * (K_A + K_B – S)$

$DIFF = K_F - K_S$

$Q = (B_{max}k_1[L](10^{-9}))/DIFF$

Where [RL] is the amount of receptor-ligand complex, [L] is the concentration [^{3}H]CP55940 in nM per experiment (~1.5 nM), [I] depicts the used concentration of unlabeled competitor in nM, K_A and K_B are the observed association rates (k_{obs}) of [^{3}H]CP55940 and the unlabeled competitor, respectively, k_1 and k_3 the association rate constants (k_{on} in $M^{-1}min^{-1}$) of [^{3}H]CP55940 (determined per experiment)

and the unlabeled competitor, respectively, k_2 and k_4 the dissociation rate constants (k_{off} in min^{-1}) of [^{3}H]CP55940 (0.0115 min^{-1}, determined using three independent dissociation experiments) and the unlabeled competitor, respectively and t is the time in minutes. The k_{on} ($M^{-1}min^{-1}$) and k_{off} (min^{-1}) provided by Prism were converted manually to k_{on} ($M^{-1}s^{-1}$) and k_{off} (s^{-1}). Receptor residence time (RT, in min) was calculated by taking the reciprocal of the dissociation rate as follows room temperature = $1/(60*k_{off})$, as k_{off} is in s^{-1}. ß-Arrestin recruitment and GTPγS data were analyzed by Prism's nonlinear regression analysis "log (agonist) vs. response – variable slope" to obtain potency (EC_{50}) and efficacy (E_{max}) values of ligands. The efficacy of all agonists was normalized to the effects of 10 µM CP55940. The bottom of the curves were constrained at 0. All data was obtained from three separate experiments performed in duplicate, unless stated otherwise. The correlation between two independent variables or data sets was calculated using a two-tailed Pearson correlation analysis.[35] A P-value of less than 0.05 was considered significant.

3. Results

3.1 Equilibrium binding affinity of the LEI101-library

The affinities of the 24 newly synthesized compounds were determined in a radioligand displacement assay using [^{3}H]CP55940 as the radiolabeled competitor at a temperature of 25°C. The structure, affinity (pK_i) and physicochemical properties of the library are presented in **Table 1**. All compounds showed concentration-dependent displacement of [^{3}H]CP55940. Compounds **6**, **7**, **8**, **17**, **21**, **22** and **23**, carrying a propyl or isobutyl group at the R^2 position, displayed the highest affinities within the library (pK_i > 7.5). In contrast, compounds **3**, **11**, **16**, and **20**, carrying a more bulky methoxyethyl or butyl group at the R^2 position, displayed ~10- to 100-fold lower affinities, ranging from 5.35 ± 0.04 (compound **11**) to 6.56 ± 0.13 (compound **20**). Compounds **1**, **9** and **18**, without a substituent at R^2, had the lowest affinities (pK_i = ~5.5) of the library. On the R^1 position, compounds with a morpholine substituent (compounds **10**-**17**) or a piperazine (compound **24**) generally had lower affinities

compared to corresponding dioxidethiomorpholino agonists with the same substituent at the R^2 position (e.g. compound **11** vs. **2** and **20**, **12** vs. **3** and **21** or **15** vs. **6** and **24**).

3.2 High throughput kinetic screening of LEI101-library

Next, the binding kinetics of all compounds were determined using the high throughput dual-point competition association assay, yielding Kinetic Rate Index (KRI) values that describe the relative (dissociation) kinetics of the agonist library compared to the radioligand used, [^{3}H]CP55940. These experiments, and all the following kinetic experiments, were performed at a reduced temperature of 10°C to increase the 'resolution' of the assay, enabling us to examine the influence of different physicochemical properties on the relative binding kinetics of the compounds within the library. Firstly, we validated that the affinities of the molecules were similar (particularly in rank order) at 10°C as compared to 25°C using a selection of 8 representative agonists with low, moderate and high affinity (data not shown). Subsequently, we used a single concentration of the compounds (1.0 x IC_{50}) for determination of the KRI values (**Table 1**). Most compounds had a KRI value lower than 1.0, which indicates a residence time (RT) shorter than that of [^{3}H]CP55940. Compounds **2**, **4** and **6** had the lowest KRI values (0.53 ± 0.06, 0.52 ± 0.09 and 0.51 ± 0.05, respectively), whereas only **7**, **22** and **23** had a KRI value larger than 1.0 (1.06 ± 0.11, 1.21 ± 0.07 and 1.03 ± 0.08, respectively). These three compounds all have an isobutyl moiety at the R^2 position, the most lipophilic substituent in this series, but have different R^1 substituents, a dioxidethiomorpholine (**7**), a piperidine (**22**), or a methylpiperidine (**23**).

3.3 Full kinetic profiling of the LEI101-library

Based on the results from the KRI screen, twelve agonists were selected for further kinetic characterization. These compounds contained a dioxidethiomorpholine at the R^1 position (group A, compounds **1**-**7**) or an isobutyl group at the R^2 position (group B, compounds **7**, **8**, **15**, **17**, **22**, **23**). Of note, compound **7** belongs to both groups. The molecules comprised a wide range of KRI values between 0.51 and 1.21, respectively the lowest and highest KRI measured in this agonist library. Together this allowed a comprehensive investigation of structure-kinetic relationships at the CB_2R. We used a competition association assay with [^{3}H]CP55940 that yielded the association- and dissociation rate constants (k_{on} and k_{off} values, respectively) of the compounds (**Table 2**). A significant correlation between the KRI values and k_{off} values was found (**Figure 3A**). The association of [^{3}H]CP55940 alone and in presence of a fast dissociating compound (**2**; KRI = 0.53 ± 0.06) and a slow dissociating compound (**7;** KRI = 1.06 ± 0.11) is shown in **Figure 3B**. The association of [^{3}H]CP55940 (k_{off} = 1.9 ± 0.1 x 10^{-4} s^{-1}, data not shown) in competition with **7** (k_{off} = 2.4 ± 0.1 x 10^{-4} s^{-1}), resulted in a small overshoot after which it reached a plateau at ~20%. In contrast, association of [^{3}H]CP55940 in competition with **2** (k_{off} = 1.2 ± 0.6 x 10^{-2} s^{-1}) resulted in a gradual increase of [^{3}H]CP55940 binding over time. The k_{on} values varied between 2.2 ± 1.0 x 10^3 M^{-1} s^{-1} (**1**) and 1.9 ± 0.8 x 10^5 M^{-1} s^{-1} (**15**). Moreover, the variety in k_{on} and k_{off} values was visualized using a kinetic map (**Figure 3C**), created by plotting the k_{on} values against k_{off} values. The diagonals represent the 'kinetic' K_D value (K_D = k_{off}/k_{on}) and show that compounds with similar K_D values can have different combinations of k_{off} and k_{on} values. For example, **2** and LEI101 (**4**) have a similar K_D value (K_D = 10^{-7} M), but have a more than 0.5 log-difference both in k_{off} and k_{on} values. Of note, compounds with a $K_D \leq 10^{-8}$ M (black circle) all have dissociation rates slower than 10^{-3} s^{-1}, while compounds with a dissociation rate

between 10^{-3} and 10^{-2} s^{-1} (dashed circle) predominantly had a K_D between 10^{-7} and 10^{-8} M, due to a small variety in their k_{on} values. Of note, **1** (R^2 = H) had a 10-fold smaller k_{on} value compared to the other compounds, thereby making it an outlier in the kinetic map (**Figure 3C**).

The kinetic K_D values of all compounds (**Table 2**) were compared to the equilibrium affinities (K_i values) (**Figure 4A**). A statistically significant correlation was found between the negative logarithm of the kinetic K_D (10°C) and the equilibrium pK_i (25°C). Of note, the pK_D values were all 0.5 log unit (~3-fold) higher than the pK_i values. A correlation between pK_D and k_{off} or residence time was also identified (**Figure 4B,C**), but not between pK_D and k_{on} values (**Figure 4D**).

3.4 Structure-Kinetics Relationships

The kinetic profile of the compounds was used to derive structure-kinetics relationships. The longest residence times (RT > 30 min) were displayed by compounds with a propyl (**6**, RT = 32 ± 9 min) or isobutyl group at the R^2 position (**7**, **8**, **17**, **22** and **23**, RT = 71 ± 3, 37 ± 5, 72 ± 8, 69 ± 2 and 31 ± 6 min, respectively). Compounds **2** and **3** displayed the shortest residence times (RT = 2.2 ± 0.8 and 3.6 ± 1.5 min, respectively). Interestingly, the residence time of **1** was similar as LEI101 (**4**) (RT = 14 ± 6 and 8.8 ± 1.6 min for **1** and **4**, respectively), despite a 10-fold lower binding affinity (pK_i = 5.55 ± 0.08 and 6.51 ± 0.09 for **1** and **4**, respectively), which was due to the very low k_{on} value of **1** (2.2 ± 1.0 x 10^3 $M^{-1}s^{-1}$).

3.5 Influence of physicochemical properties on affinity and binding kinetics

Next, we analyzed the effects of physicochemical properties on equilibrium affinity and binding kinetics. Hence, the cLogP (**Table 1**) of the compounds with varying alkyl

R^2 substituents (group A) and the basicity (pK_a) with varying amine R^1 substituents (group B) were plotted against equilibrium affinity, association rate k_{on} and residence time. The basicity of group B did not correlate with any of the measured parameters (pK_i: Pearson r: 0.02328, *p*-value = 0.9064; k_{on}: Pearson r: -0.2213, *p*-value = 0.6735; RT: Pearson r: 0.3944, *p*-value = 0.5112; graphs not shown). In case of group A, a near-significant correlation was identified with their lipophilicity and equilibrium affinity (Pearson r: 0.692, *p*-value = 0.0542, **Figure 5A**), but not with k_{on} (Pearson r: 0.1452, *p*-value = 0.7561, **Figure 5B**). Interestingly, cLogP of group A was highly correlated with residence time (Pearson r: 0.8869, *p*-value = 0.0078, **Figure 5C**). Noteworthy, this correlation was not observed with the R^1 substituents of group B (**Figure 6**).

3.6 Influence of binding kinetics on functional activity

Finally, the influence of residence time on functional activity of the compound library was investigated. To this end, both groups were characterized in two functional assays: GTPγS binding and β-arrestin recruitment (**Table 2**). All compounds displayed partial agonism in both assays relative to CP55940. The highest intrinsic efficacy was observed for **5** in the G protein activation assay (E_{max} = 79 ± 14%), whereas agonist **2** had the highest efficacy in the β-arrestin recruitment assay (E_{max} = 76 ± 15%). The lowest efficacy was observed for **1** in both functional assays (β-arrestin: E_{max} = 25 ± 2%; GTPγS: E_{max} = 48 ± 7%). Generally, agonists showed a lower efficacy for β-arrestin recruitment, except for agonists **2**, **6** and **15** (E_{max} β-arrestin: 76 ± 15, 62 ± 8 and 64 ± 10 compared to E_{max} GTPγS: 54 ± 13, 50 ± 2 and 65 ± 12, respectively), although these differences were not significant. Indeed, no correlation was observed between the efficacies of the compounds in the two functional assays (Pearson r: 0.4247, *p*-value = 0.1688, correlation graphs not

shown). In addition, no correlation between residence time and *in vitro* efficacy was identified (GTPγS Pearson r: 0.00621, *p*-value: 0.9895; β-arrestin Pearson r: 0.1053, *p*-value 0.8222, graphs not shown). For example, the long residence time of agonists **6**, **7**, **8**, **17**, **22** and **23** did not have a higher efficacy than the other agonists in either functional assay. In fact, agonist **2** with the shortest residence time (2.2 ± 0.8 min) had a very moderate efficacy in GTPγS (54 ± 13%), and the highest efficacy of all agonists for β-arrestin recruitment (76 ± 15%).

The potencies ranged from 6.06 ± 0.27 (**3**) to 7.94 ± 0.24 (**7**) in the GTPγS assay, whereas in the β-arrestin recruitment assay the potencies ranged from 6.12 ± 0.23 (**1**) to 8.14 ± 0.08 (**22**). In contrast to efficacy, the potency of the compounds was similar and highly correlated in the two functional assays (Pearson r: 0.8445, *p*-value < 0.0005). In general the compounds showed a higher potency in β-arrestin recruitment assays. For example, **22** showed a 17-fold higher potency for β-arrestin recruitment compared to G protein activation (pEC_{50} = 8.14 ± 0.08 and 6.91 ± 0.32, respectively).

Notably, nanomolar potency (pEC_{50} > 7.5) was only displayed by agonists with a residence time of at least 30 min as exemplified by compounds **6**, **8** and **23** (with residence times of 32 ± 9, 37 ± 5 and 31 ± 6 min, respectively) and compounds **7**, **17** and **22** (RT = 71 ± 3, 72 ± 8 and 69 ± 2 min, respectively). A statistically significant correlation was found of the residence times of group A with functional potency for both G protein activation and β-arrestin recruitment (**Figure 7A-B**). Interestingly, the residence times of group B did not correlate with either potency or efficacy (GTPγS E_{max} Pearson r: 0.0021, *p*-value: 0.9968; pEC_{50} Pearson r: 0.3391, *p*-value: 0.5108; β-arrestin E_{max} Pearson r: -0.2591, *p*-value: 0.6200; pEC_{50} Pearson r: 0.6586, *p*-value: 0.1549, graphs not shown).

4. Discussion

4.1 Kinetic characterization of LEI101-based agonists

Recently, drug discovery research has focused on the development of selective CB_2R agonists for the treatment of tissue injury and inflammatory diseases that avoid inducing CB_1R-mediated psychoactive side effects. CB_2R knockout mice show enhanced pathology in various inflammatory disease models, including heart, liver or kidney injury and inflammatory pain, thereby supporting the notion that CB_2R plays an essential role in these conditions. Despite compelling proof-of-concept data obtained in preclinical pain models, several CB_2R agonists lacked efficacy in phase 2 clinical trials for unknown reasons.[29, 36]

Drug-target binding kinetics and their influence on functional activity are increasingly considered in drug discovery because it may aid in the design of lead compounds.[2] Therefore, we have investigated the relationships between functional activity and binding kinetics of a series of agonists, based on the CB_2R-selective agonist LEI101, which showed *in vivo* efficacy in the treatment of neuropathic pain and inflammation-induced tissue damage.[26, 27]

In this study, radioligand binding assays were performed with [^{3}H]CP55940, an agonistic radioligand commonly used to determine CBR pharmacology,[37] including binding kinetics.[38, 39] Recently, Sykes *et al.* showed the importance of using physiological concentrations of sodium when determining binding kinetics at the muscarinic M3 receptor.[40] However, in this study sodium ions were absent in all assays where the agonist [^{3}H]CP55940 was used to prevent that the receptor population was forced into a predominantly inactive state, i.e. for which an agonist would have a low affinity.[41] In addition, in our system we have never observed a

biphasic interaction for agonists, which would prohibit the use of the the Motulsky-Mahan mathematical model as it describes binding of a ligand to a single site, e.g. receptor.[34, 42] Hence, we also did not apply GTP to force the receptor population in a single (inactive) state. Importantly, we believe that it is unlikely that the omission of sodium salts and/or GTP would result in a different rank order of binding kinetics of the agonist library. This line of thought is further corroborated by the study on tiotropium and NVA237 in presence of sodium ions that resulted in shorter residence times, but the same rank order.[40]

The measured equilibrium binding affinities corresponded to previously determined structure-activity relationships (SAR) for this scaffold.[27] Using a high-throughput kinetic screening assay, based on its equivalent for the Adenosine A_1 receptor,[28] agonists with R^1 = dioxidethiomorpholine (group A) and R^2 = isobutyl (group B) were selected for full kinetic characterization (**Figure 3A**). We found that the kinetic profile of the agonists had smaller variations in k_{on} values, but larger variations in k_{off} values, which were visualized using a kinetic map of the agonist library (**Figure 3C**). For this series of compounds, binding affinity was mostly influenced by their dissociation rate, as illustrated by a significant correlation with k_{off} values, but not with k_{on} values. (**Figure 4C,D**). This observation was similar as reported for the the adenosine A_{2A} receptor,[16, 17] but in contrast to reports on β_2 adrenergic receptors and the hERG channel, for which the association rate was found to be the main driving force in ligand affinity.[43, 44]

4.2 The role of physicochemical properties on binding kinetics and functional activity

Previously, it has been shown that controlling physicochemical properties such as lipophilicity and basicity can lead to 'tuned drug-target binding kinetics.[8, 45, 46] Therefore we divided our library into two groups in which we systematically varied either the lipophilicity or the basicity at different locations of the scaffold. This way, we could investigate the relationships between physicochemical properties, binding kinetics and functional activity of these agonists, for which two independent signaling pathways were used; G protein activation and β-arrestin recruitment.

A significant correlation was found between increasing lipophilicity at the R^2 position of the LEI101 scaffold and residence time (group A agonists, **Figure 5C**), but not for the R^1 position (group B agonists, **Figure 6**). By dividing our compound library in two parts, we showed that there is a lipophilic binding domain in the receptor targeted by the R^2 substituents. Occupying this pocket increases binding affinity due to decreased dissociation rate. Hence, it is not the overall lipophilicity of a molecule that determines its dissociation rate, but rather the lipophilicity at a specific position of the scaffold.[45] These findings fit well with the observation that any relationships between physicochemical properties and binding kinetics are both ligand and target specific and constitute the molecular underpinning of the lipophilic efficiency index.[47]

Currently, there is no CB_2R crystal structure available to validate the positioning of this lipophilic binding domain, but a lipophilic binding domain was identified in the active site of CB_1R, formed by six amino acid residues,[48, 49] of which four (i.e. Val114$^{3.32}$, Tyr191$^{5.39}$, Leu192$^{5.40}$ and Met275$^{6.55}$) are conserved in the CB_2R active site.[50] This indicates that these residues may also play a role in the formation of a lipophilic binding domain responsible for the increased residence time of LEI101-based agonists with lipophilic R^2 substituents.

All compounds were identified as partial agonists in two signaling pathways, G protein activation and β-arrestin recruitment relative to CP55940 that behaved as a full agonist.[51] From these so-called 'end-point' assays no obvious biased agonism was observed, although these molecules have different binding kinetics. However, follow up studies with regard to the influence of assay time and readout should be performed to investigate the role of kinetic context on biased agonism.[52] On a similar note, these functional assays were performed at different temperatures (i.e. 25°C and 37°C), which may influence the potency and efficacy values of the compounds tested. Although this will probably not result in a difference in rank order, it may influence the observed lack of biased signaling.[52]

Interestingly, nanomolar potency for G protein activation and β-arrestin recruitment was associated with compounds having a residence time longer than 30 min, as a significant correlation between dissociation rate and functional potency for both assays was identified (**Figure 7**). Again, this observation was specific for group A agonists. No correlation between residence time and functional efficacy was identified, as was reported for the Adenosine A_1 receptor.[53] This observation is in contrast with the previously reported positive correlation found between residence time and efficacy, but not potency, for the Adenosine A_{2A} receptor and Muscarinic M3 receptor.[16] Of note, for the Adenosine A_{2A} receptor these molecules showed significant longer residence times than the LEI101-based agonist library.

4.3 Target-specific binding kinetics in drug discovery

Previously, the CB_2R binding kinetics of CP55940, as well as some other synthetic cannabinoid ligands (e.g. JWH133, HU308) and endocannabinoids were reported.[42] Because CP55940 was measured in both studies, we could use its

binding kinetics as reference to compare the binding kinetics of the ligands tested in the two different studies. Interestingly, the kinetic profile of this agonist library shows remarkable differences compared to the reported binding kinetics of some structurally different synthetic ligands for CB_2R, like JWH133 and SR144528 and endocannabinoids anandamide (AEA) and noladin ether (NE), which all had divergent, but relatively fast kinetics.[54] For these molecules, the association rate was the main driving force for their affinity. Knowledge of the kinetic binding parameters of a target's endogenous ligands is important for two reasons: 1) it is an indication of the ligand binding kinetics necessary to maintain homeostasis and 2) these play a major role in defining the pharmacological effect of a drug, as they have to compete with the endogenous ligands for binding to the active site.[55, 56] Notably, LEI101, identified to be *in vivo* active in the treatment of neuropathic pain and inflammation-induced tissue damage,[26, 27] has similar binding kinetics as 2-AG, relative to CP55940 (10-fold slower k_{on}, 10-fold faster k_{off}).[54] This may indicate that slow association plays a role in the *in vivo* efficacy of LEI101. Interestingly, HU308 and JWH133, also *in vivo* active CB_2R-selective agonists,[29, 57, 58] had slower association rates,[54] but a similar dissociation rate, relative to CP55940 (20-50-fold slower k_{on}, similar k_{off}). This may indicate that the optimal kinetic profile of *in vivo* active CB_2R agonists is flexible, or may be dependent on disease type and/or progression. Although, it is noted that species differences between mouse and human CB_2R have not been taken into account.

Interestingly, slowly associating ligands may decrease on-target related side effects by preventing high target occupancy and fast target activation.[14] This could be important, because prolonged activation of CB_2R is hypothesized to interfere with the ECS homeostasis.[54],[59] Specifically, local, transient activation of CB_2R by

endocannabinoids may lead to immunosuppression in the early phases of the immune response, perhaps via apoptotic mechanisms.[60, 61] Rapid restoration of cellular activity might also be required to counteract potential infectious threats.[62] This indicates that the optimal kinetic profile of novel molecules needs to be established according to their functional activity, and should always be a combination of association and dissociation rates, resulting in an optimal level of receptor occupancy *in vivo*.[63]

4.4 Conclusion

In summary, we have reported the structure kinetics relationship of LEI101-based agonists of the cannabinoid CB_2 receptor. We identified the lipophilicity of R^2 position as important feature to increase receptor residence time, which correlated with increased potency, but not with efficacy, in two signaling pathways: G protein activation and β-arrestin recruitment. The findings of this study provide important insights into how CB_2R agonists can be designed with desired kinetic profiles for the future development of novel treatments of inflammatory diseases.

Acknowledgments

This work was supported by an ECHO-STIP grant from the Netherlands Organisation for Scientific Research. The authors would like to thank Hans van den Elst, Fons Lefeber and Karthick Babu Sai Sankar Gupta for technical assistance with HRMS and NMR measurements, respectively.

Conflicts of interest

None

Authorship contributions

Participated in research design: Soethoudt, van der Stelt, Heitman

Conducted experiments: Soethoudt, Hoorens, Doelman, Martella

Performed data analysis: Soethoudt, Hoorens, Doelman

Wrote or contributed to the writing of the manuscript: Soethoudt, van der Stelt, Heitman

References

[1] R. Zhang, F. Monsma, Binding kinetics and mechanism of action: toward the discovery and development of better and best in class drugs, Expert Opin Drug Discov 5(11) (2010) 1023-9.
[2] R.A. Copeland, D.L. Pompliano, T.D. Meek, Drug-target residence time and its implications for lead optimization, Nat Rev Drug Discov 5(9) (2006) 730-9.
[3] H. Lu, K. England, C.A. Ende, J.J. Truglio, S. Luckner, B.G. Reddy*, et al.*, Slow-Onset Inhibition of the FabI Enoyl Reductase from Francisella tularensis: Residence Time and in Vivo Activity, Acs Chemical Biology 4(3) (2009) 221-231.
[4] F. Daryaee, A. Chang, J. Schiebel, Y. Lu, Z. Zhang, K. Kapilashrami*, et al.*, Correlating drug-target kinetics and in vivo pharmacodynamics: long residence time inhibitors of the FabI enoyl-ACP reductase, Chem Sci 7(9) (2016) 5945-5954.
[5] L.T. Gooljarsingh, C. Fernandes, K. Yan, H. Zhang, M. Grooms, K. Johanson*, et al.*, A biochemical rationale for the anticancer effects of Hsp90 inhibitors: slow, tight binding inhibition by geldanamycin and its analogues, Proc Natl Acad Sci U S A 103(20) (2006) 7625-30.
[6] R.A. Copeland, J.M. Williams, J. Giannaras, S. Nurnberg, M. Covington, D. Pinto*, et al.*, Mechanism of selective inhibition of the inducible isoform of prostaglandin G/H synthase, Proc Natl Acad Sci U S A 91(23) (1994) 11202-6.
[7] R.A. Copeland, The drug-target residence time model: a 10-year retrospective, Nat Rev Drug Discov 15(2) (2016) 87-95.
[8] D. Guo, J.M. Hillger, I.J. AP, L.H. Heitman, Drug-target residence time--a case for G protein-coupled receptors, Med Res Rev 34(4) (2014) 856-92.
[9] G. Vauquelin, S.J. Charlton, Long-lasting target binding and rebinding as mechanisms to prolong in vivo drug action, Brit J Pharmacol 161(3) (2010) 488-508.
[10] K.P. Cusack, Y. Wang, M.Z. Hoemann, J. Marjanovic, R.G. Heym, A. Vasudevan, Design strategies to address kinetics of drug binding and residence time, Bioorg Med Chem Lett 25(10) (2015) 2019-27.
[11] G.S. Van Aller, M.B. Pappalardi, H.M. Ott, E. Diaz, M. Brandt, B.J. Schwartz*, et al.*, Long residence time inhibition of EZH2 in activated polycomb repressive complex 2, ACS Chem Biol 9(3) (2014) 622-9.
[12] M.R. Dowling, S.J. Charlton, Quantifying the association and dissociation rates of unlabelled antagonists at the muscarinic M3 receptor, Br J Pharmacol 148(7) (2006) 927-37.

[13] G. Vauquelin, S. Bostoen, P. Vanderheyden, P. Seeman, Clozapine, atypical antipsychotics, and the benefits of fast-off D2 dopamine receptor antagonism, Naunyn Schmiedebergs Arch Pharmacol 385(4) (2012) 337-72.
[14] D.A. Sykes, H. Moore, L. Stott, N. Holliday, J.A. Javitch, J.R. Lane*, et al.*, Extrapyramidal side effects of antipsychotics are linked to their association kinetics at dopamine D-2 receptors, Nature Communications 8 (2017).
[15] W.E.A. de Witte, M. Danhof, P.H. van der Graaf, E.C.M. de Lange, In vivo Target Residence Time and Kinetic Selectivity: The Association Rate Constant as Determinant, Trends in Pharmacological Sciences 37(10) (2016) 831-842.
[16] D. Guo, T. Mulder-Krieger, I.J. AP, L.H. Heitman, Functional efficacy of adenosine A(2)A receptor agonists is positively correlated to their receptor residence time, Br J Pharmacol 166(6) (2012) 1846-59.
[17] D.A. Sykes, M.R. Dowling, S.J. Charlton, Exploring the mechanism of agonist efficacy: a relationship between efficacy and agonist dissociation rate at the muscarinic M3 receptor, Molecular pharmacology 76(3) (2009) 543-51.
[18] C.S. Tautermann, T. Kiechle, D. Seeliger, S. Diehl, E. Wex, R. Banholzer*, et al.*, Molecular Basis for the Long Duration of Action and Kinetic Selectivity of Tiotropium for the Muscarinic M3 Receptor, Journal of Medicinal Chemistry 56(21) (2013) 8746-8756.
[19] A. Ligresti, L. De Petrocellis, V. Di Marzo, From Phytocannabinoids to Cannabinoid Receptors and Endocannabinoids: Pleiotropic Physiological and Pathological Roles Through Complex Pharmacology, Physiol Rev 96(4) (2016) 1593-659.
[20] K. Mackie, Cannabinoid receptor homo- and heterodimerization, Life Sci 77(14) (2005) 1667-73.
[21] R. Mechoulam, L.O. Hanus, R. Pertwee, A.C. Howlett, Early phytocannabinoid chemistry to endocannabinoids and beyond, Nat Rev Neurosci 15(11) (2014) 757-64.
[22] B.K. Atwood, A. Straiker, K. Mackie, CB(2): therapeutic target-in-waiting, Prog Neuropsychopharmacol Biol Psychiatry 38(1) (2012) 16-20.
[23] S. Galiegue, S. Mary, J. Marchand, D. Dussossoy, D. Carriere, P. Carayon*, et al.*, Expression of central and peripheral cannabinoid receptors in human immune tissues and leukocyte subpopulations, Eur J Biochem 232(1) (1995) 54-61.
[24] P. Pacher, R. Mechoulam, Is lipid signaling through cannabinoid 2 receptors part of a protective system?, Prog Lipid Res 50(2) (2011) 193-211.
[25] J. Guindon, A.G. Hohmann, Cannabinoid CB2 receptors: a therapeutic target for the treatment of inflammatory and neuropathic pain, Br J Pharmacol 153(2) (2008) 319-34.
[26] P. Mukhopadhyay, M. Baggelaar, K. Erdelyi, Z. Cao, R. Cinar, F. Fezza*, et al.*, The novel, orally available and peripherally restricted selective cannabinoid CB2 receptor agonist LEI-101 prevents cisplatin-induced nephrotoxicity, Br J Pharmacol 173(3) (2016) 446-58.
[27] M. van der Stelt, J. Cals, S. Broeders-Josten, J. Cottney, A.A. van der Doelen, M. Hermkens*, et al.*, Discovery and optimization of 1-(4-(pyridin-2-yl)benzyl)imidazolidine-2,4-dione derivatives as a novel class of selective cannabinoid CB2 receptor agonists, J Med Chem 54(20) (2011) 7350-62.
[28] D. Guo, E.J. van Dorp, T. Mulder-Krieger, J.P. van Veldhoven, J. Brussee, A.P. Ijzerman*, et al.*, Dual-point competition association assay: a fast and high-throughput kinetic screening method for assessing ligand-receptor binding kinetics, J Biomol Screen 18(3) (2013) 309-20.

[29] M. Soethoudt, U. Grether, J. Fingerle, T.W. Grim, F. Fezza, L. de Petrocellis*, et al.*, Cannabinoid CB2 receptor ligand profiling reveals biased signalling and off-target activity, Nat Commun 8 (2017) 13958.
[30] P.K. Smith, R.I. Krohn, G.T. Hermanson, A.K. Mallia, F.H. Gartner, M.D. Provenzano*, et al.*, Measurement of protein using bicinchoninic acid, Anal Biochem 150(1) (1985) 76-85.
[31] C. Harrison, J.R. Traynor, The [35S]GTPgammaS binding assay: approaches and applications in pharmacology, Life Sci 74(4) (2003) 489-508.
[32] M. Soethoudt, N. van Gils, M. van der Stelt, L.H. Heitman, Protocol to Study beta-Arrestin Recruitment by CB1 and CB2 Cannabinoid Receptors, Methods Mol Biol 1412 (2016) 103-11.
[33] Y. Cheng, W.H. Prusoff, Relationship between the inhibition constant (K1) and the concentration of inhibitor which causes 50 per cent inhibition (I50) of an enzymatic reaction, Biochem Pharmacol 22(23) (1973) 3099-108.
[34] H.J. Motulsky, L.C. Mahan, The kinetics of competitive radioligand binding predicted by the law of mass action, Molecular pharmacology 25(1) (1984) 1-9.
[35] K. Pearson, Determination of the Coefficient of Correlation, Science 30(757) (1909) 23-5.
[36] T. Ostenfeld, J. Price, M. Albanese, J. Bullman, F. Guillard, I. Meyer*, et al.*, A randomized, controlled study to investigate the analgesic efficacy of single doses of the cannabinoid receptor-2 agonist GW842166, ibuprofen or placebo in patients with acute pain following third molar tooth extraction, Clin J Pain 27(8) (2011) 668-76.
[37] A. Cooper, S. Singh, S. Hook, J.D.A. Tyndall, A.J. Vernall, Chemical Tools for Studying Lipid-Binding Class A G Protein-Coupled Receptors, Pharmacological reviews 69(3) (2017) 316-353.
[38] L. Xia, H. de Vries, E.B. Lenselink, J. Louvel, M.J. Waring, L. Cheng*, et al.*, Structure-Affinity Relationships and Structure-Kinetic Relationships of 1,2-Diarylimidazol-4-carboxamide Derivatives as Human Cannabinoid 1 Receptor Antagonists, Journal of medicinal chemistry 60(23) (2017) 9545-9564.
[39] L. Xia, H. de Vries, X. Yang, E.B. Lenselink, A. Kyrizaki, F. Barth*, et al.*, Kinetics of human cannabinoid 1 (CB1) receptor antagonists: Structure-kinetics relationships (SKR) and implications for insurmountable antagonism, Biochem Pharmacol (2017).
[40] D.A. Sykes, M.R. Dowling, J. Leighton-Davies, T.C. Kent, L. Fawcett, E. Renard*, et al.*, The Influence of receptor kinetics on the onset and duration of action and the therapeutic index of NVA237 and tiotropium, The Journal of pharmacology and experimental therapeutics 343(2) (2012) 520-8.
[41] V. Katritch, G. Fenalti, E.E. Abola, B.L. Roth, V. Cherezov, R.C. Stevens, Allosteric sodium in class A GPCR signaling, Trends in Biochemical Sciences 39(5) (2014) 233-44.
[42] A. Martella, H. Sijben, A.C. Rufer, U. Grether, J. Fingerle, C. Ullmer*, et al.*, A Novel Selective Inverse Agonist of the CB2 Receptor as a Radiolabeled Tool Compound for Kinetic Binding Studies, Molecular pharmacology 92(4) (2017) 389-400.
[43] D.A. Sykes, S.J. Charlton, Slow receptor dissociation is not a key factor in the duration of action of inhaled long-acting ss(2)-adrenoceptor agonists, Brit J Pharmacol 165(8) (2012) 2672-2683.
[44] Z. Yu, J.P.D. van Veldhoven, J. Louvel, I.M.E. 't Hart, M.B. Rook, M.A.G. van der Heyden*, et al.*, Structure-Affinity Relationships (SARs) and Structure-Kinetics Relationships (SKRs) of K(v)11.1 Blockers, Journal of Medicinal Chemistry 58(15) (2015) 5916-5929.

[45] D.C. Miller, G. Lunn, P. Jones, Y. Sabnis, N.L. Davies, P. Driscoll, Investigation of the effect of molecular properties on the binding kinetics of a ligand to its biological target, Medchemcomm 3(4) (2012) 449-452.
[46] G. Tresadern, J.M. Bartolome, G.J. Macdonald, X. Langlois, Molecular properties affecting fast dissociation from the D2 receptor, Bioorg Med Chem 19(7) (2011) 2231-41.
[47] D. Guo, L.Z. Xia, J.P.D. van Veldhoven, M. Hazeu, T. Mocking, J. Brussee*, et al.*, Binding Kinetics of ZM241385 Derivatives at the Human Adenosine A(2A) Receptor, Chemmedchem 9(4) (2014) 752-761.
[48] T. Hua, K. Vemuri, S.P. Nikas, R.B. Laprairie, Y. Wu, L. Qu*, et al.*, Crystal structures of agonist-bound human cannabinoid receptor CB1, Nature 547(7664) (2017) 468-+.
[49] L. Xia, H. de Vries, E.B. Lenselink, J. Louvel, M.J. Waring, L. Cheng*, et al.*, Structure–Affinity Relationships and Structure–Kinetic Relationships of 1,2-Diarylimidazol-4-carboxamide Derivatives as Human Cannabinoid 1 Receptor Antagonists, Journal of Medicinal Chemistry (2017).
[50] R.D. Zhang, D.P. Hurst, J. Barnett-Norris, P.H. Reggio, Z.H. Song, Cysteine 2.59(89) in the second transmembrane domain of human CB2 receptor is accessible within the ligand binding crevice: Evidence for possible CB2 deviation from a rhodopsin template, Molecular Pharmacology 68(1) (2005) 69-83.
[51] G. Griffin, P.J. Atkinson, V.M. Showalter, B.R. Martin, M.E. Abood, Evaluation of cannabinoid receptor agonists and antagonists using the guanosine-5 '-O-(3-[S-35]thio)-triphosphate binding assay in rat cerebellar membranes, Journal of Pharmacology and Experimental Therapeutics 285(2) (1998) 553-560.
[52] C. Klein Herenbrink, D.A. Sykes, P. Donthamsetti, M. Canals, T. Coudrat, J. Shonberg*, et al.*, The role of kinetic context in apparent biased agonism at GPCRs, Nat Commun 7 (2016) 10842.
[53] J. Louvel, D. Guo, M. Agliardi, T.A.M. Mocking, R. Kars, T.P. Pham*, et al.*, Agonists for the Adenosine A(1) Receptor with Tunable Residence Time. A Case for Nonribose 4-Amino-6-aryl-5-cyano-2-thiopyrimidines, Journal of Medicinal Chemistry 57(8) (2014) 3213-3222.
[54] A. Martella, H. Sijben, A. Rufer, J. Fingerle, U. Grether, C. Ullmer*, et al.*, A novel selective inverse agonist of the CB2 receptor as a radiolabeled tool compound for kinetic binding studies, Mol Pharmacol (2017).
[55] I. Nederpelt, D. Bleeker, B. Tuijt, I.J. AP, L.H. Heitman, Kinetic binding and activation profiles of endogenous tachykinins targeting the NK1 receptor, Biochem Pharmacol 118 (2016) 88-95.
[56] I. Nederpelt, M. Kuzikov, W.E.A. de Witte, P. Schnider, B. Tuijt, S. Gul*, et al.*, From receptor binding kinetics to signal transduction; a missing link in predicting in vivo drug-action, Sci Rep-Uk 7 (2017).
[57] H.P. Xu, C.L. Cheng, M. Chen, A. Manivannan, L. Cabay, R.G. Pertwee*, et al.*, Anti-inflammatory property of the cannabinoid receptor-2-selective agonist JWH-133 in a rodent model of autoimmune uveoretinitis, J Leukocyte Biol 82(3) (2007) 532-541.
[58] M. Rajesh, H. Pan, P. Mukhopadhyay, S. Batkai, D. Osei-Hyiaman, G. Hasko*, et al.*, Pivotal Advance: Cannabinoid-2 receptor agonist HU-308 protects against hepatic ischemia/reperfusion injury by attenuating oxidative stress, inflammatory response, and apoptosis, J Leukocyte Biol 82(6) (2007) 1382-1389.

[59] V. Di Marzo, The endocannabinoid system: its general strategy of action, tools for its pharmacological manipulation and potential therapeutic exploitation, Pharmacol Res 60(2) (2009) 77-84.
[60] A.C. Herring, W.S. Koh, N.E. Kaminski, Inhibition of the cyclic AMP signaling cascade and nuclear factor binding to CRE and kappa B elements by cannabinol, a minimally CNS-Active cannabinoid, Biochemical Pharmacology 55(7) (1998) 1013-1023.
[61] T.K. Eisenstein, J.J. Meissler, Q. Wilson, J.P. Gaughan, M.W. Adler, Anandamide and Delta(9)-tetrahydrocannabinol directly inhibit cells of the immune system via CB(2) receptors, J Neuroimmunol 189(1-2) (2007) 17-22.
[62] R. Pandey, K. Mousawy, M. Nagarkatti, P. Nagarkatti, Endocannabinoids and immune regulation, Pharmacological Research 60(2) (2009) 85-92.
[63] I. Bot, N.V. Ortiz Zacarias, W.E. de Witte, H. de Vries, P.J. van Santbrink, D. van der Velden*, et al.*, A novel CCR2 antagonist inhibits atherogenesis in apoE deficient mice by achieving high receptor occupancy, Sci Rep 7(1) (2017) 52.

Tables

Table 1. Overview of chemical structures, physicochemical properties, equilibrium affinity and Kinetic Rate Index (KRI) of the LEI101-based agonist library.

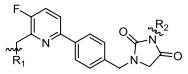

			Physicochemical properties			Binding affinity	Kinetic Rate Index
Nr.	R^1	R^2	MW (Da)	cLogP	pKa	pK_i ± SEM[a]	KRI ± SEM[b]
1		H	432	0.4	5.1	5.55 ± 0.08	0.62 ± 0.06
2			447	0.4	5.1	6.61 ± 0.18	0.53 ± 0.06
3			491	0.8	5.1	6.25 ± 0.04	0.67 ± 0.03
4 LEI101			473	0.9	5.1	6.51 ± 0.09	0.52 ± 0.09
5			461	0.9	5.1	7.06 ± 0.12	0.51 ± 0.05
6			475	1.5	5.1	7.66 ± 0.08	0.71 ± 0.05
7			489	1.9	5.1	7.74 ± 0.08	1.06 ± 0.11
8			475	4.4	6.1	7.48 ± 0.10	0.79 ± 0.05
9		H	384	1.3	6.3	5.65 ± 0.05	0.72 ± 0.08
10			398	1.4	6.3	6.06 ± 0.24	0.71 ± 0.06
11			442	1.7	6.3	5.35 ± 0.04	0.77 ± 0.05
12			424	1.9	6.3	6.17 ± 0.03	0.67 ± 0.12
13			412	1.9	6.3	6.84 ± 0.25	0.71 ± 0.08
14			426	2.4	6.3	7.13 ± 0.15	0.57 ± 0.08
15			441	2.8	6.3	7.07 ± 0.10	0.67 ± 0.05
16			440	3.0	6.3	6.21 ± 0.20	0.62 ± 0.12
17			475	3.5	6.9	7.67 ± 0.14	0.85 ± 0.13
18		H	382	2.6	8.3	5.48 ± 0.06	0.68 ± 0.07

19			396	2.6	8.3	6.70 ± 0.05	0.60 ± 0.08
20			440	3.0	8.3	6.56 ± 0.13	0.78 ± 0.05
21			425	3.7	8.3	7.92 ± 0.06	0.66 ± 0.14
22			439	4.1	8.3	7.56 ± 0.02	1.21 ± 0.07
23			453	4.6	8.3	7.61 ± 0.22	1.03 ± 0.08
24			454	3.3	8.8	5.45 ± 0.09	0.67 ± 0.01

[a] pK_i ± SEM was obtained from a [^{3}H]CP55940 equilibrium displacement assay at 25°C, on membrane fractions of CHOK1B_2R cells, and determined in three independent experiments performed in duplicate (N=3 in duplicate)

[b] KRI ± SEM was obtained from a [^{3}H]CP55940 dual point competition association assay at 10°C, on membrane fractions of CHOK1CB_2R cells (N=3 in duplicate)

Table 2. Overview of binding kinetics and functional activity in two signal transduction pathways.

		Binding kinetics				Functional activity			
						G protein activation[d]		β-arrestin recruitment[e]	
Nr.	Group	k_{off} (s^{-1})[a]	k_{on} (M^{-1} s^{-1})[a]	K_D (nM)[b]	RT (min)[c]	pEC_{50}	E_{max}	pEC_{50}	E_{max}
1	**A**	(2.7 ± 1.8) x 10^{-3}	(2.2 ± 1.0) x 10^{3}	1052 ± 264	14 ± 6	6.25 ± 0.09	48 ± 7	6.12 ± 0.23	25 ± 2
2	**A**	(1.2 ± 0.6) x 10^{-2}	(1.0 ± 0.7) x 10^{5}	155 ± 35	2.2 ± 0.8	6.18 ± 0.27	54 ± 13	6.55 ± 0.18	76 ± 15
3	**A**	(7.1 ± 3.3) x 10^{-3}	(4.4 ± 2.6) x 10^{4}	187 ± 25	3.6 ± 1.5	6.06 ± 0.27	60 ± 2	6.58 ± 0.08	45 ± 7
4 (LEI101)	**A**	(2.1 ± 0.5) x 10^{-3}	(3.0 ± 1.1) x 10^{4}	76 ± 10	8.8 ± 1.6	6.6 ± 0.2[†]	65 ± 8[†]	7.0 ± 0.3[†]	41 ± 6[†]
5	**A**	(1.5 ± 0.9) x 10^{-3}	(5.3 ± 2.6) x 10^{4}	26 ± 2	20 ± 8	6.38 ± 0.28	79 ± 14	6.76 ± 0.39	72 ± 10
6	**A**	(5.9 ± 1.3) x 10^{-4}	(6.8 ± 1.7) x 10^{4}	9 ± 2	32 ± 9	7.78 ± 0.07	50 ± 2	7.88 ± 0.10	62 ± 8
7	**A/B**	(2.4 ± 0.1) x 10^{-4}	(5.3 ± 0.4) x 10^{4}	4.5 ± 0.5	71 ± 3	7.94 ± 0.24	60 ± 6	7.83 ± 0.08	56 ± 1
8	**B**	(4.7 ± 0.1) x 10^{-4}	(5.9 ± 1.6) x 10^{4}	9 ± 1	37 ± 5	7.37 ± 0.07	61 ± 6	7.80 ± 0.07	54 ± 6
15	**B**	(4.3 ± 1.8) x 10^{-3}	(1.9 ± 0.8) x 10^{5}	24 ± 2	6.4 ± 2.9	7.18 ± 0.30	65 ± 12	7.21 ± 0.28	64 ± 10
17	**B**	(2.4 ± 0.3) x 10^{-4}	(3.7 ± 1.0) x 10^{4}	8 ± 2	72 ± 8	7.81 ± 0.15	65 ± 7	7.67 ± 0.03	53 ± 2
22	**B**	(2.4 ± 0.1) x 10^{-3}	(2.3 ± 0.3) x 10^{4}	11 ± 1	69 ± 2	6.91 ± 0.32	78 ± 9	8.14 ± 0.08	67 ± 7
23	**B**	(5.9 ± 1.3) x 10^{-4}	(7.8 ± 2.1) x 10^{4}	9 ± 2	31 ± 6	7.61 ± 0.36	77 ± 14	7.89 ± 0.21	59 ± 6

[a] k_{on} ± SEM and k_{off} ± SEM were obtained from a [^{3}H]CP55940 competition association assay at 10°C, on membrane fractions of CHOK1CB_2R cells, and determined in three independent experiments performed in duplicate (N=3 in duplicate)

[b] The K_D was calculated from k_{off} and k_{on} (N=3 in duplicate) as follows: ($K_D = k_{off}/k_{on}$)

[c] RT was calculated from k_{off} (N=3 in duplicate) as follows: ($RT=1/(60* k_{off})$)

[d] pEC_{50} ± SEM and E_{max} ± SEM were obtained from a [^{35}S]GTPγS assay at 25°C, on membrane fractions of CHOK1CB_2R cells (N=3 in duplicate)

[e] pEC_{50} ± SEM and E_{max} ± SEM were obtained from a PathHunter® β-arrestin recruitment assay at 37°C, on live CHOK1CB_2R cells (N=3 in duplicate)

Figure legends

Figure 1. Chemical structures of LEI101 (A) and the LEI101-based library of agonists 1-24 (B) synthesized in this study.

Figure 2. General procedures. Intermediates **28a-g** were obtained from a modified synthetic approach as compared to van der Stelt *et al*:[27] Starting material pyridinaldehyde **25** was reduced to primary alcohol **26**, which was mesylated to intermediate **27**. Intermediates **28a-g** were obtained by substitution with the corresponding secondary amine (R^1-H). Agonists **1**, **9** and **18** were obtained in 4 steps from intermediates **28a-c**, by Suzuki coupling, reductive amination and cyclization using an isocyanate intermediate. For the synthesis of compounds **2-8**, **10-17** and **19-24**, R^2-substituted intermediates **36a-g** were obtained in two steps from 4-bromobenzaldehyde **32**, starting with a reductive amination towards intermediates **33a** and **33b**. In case of R^2 = cyclopropyl, the R^2 substituents was introduced with a peptide coupling using cyclopropylamine, followed by cyclization to intermediate **36g**. **33a** was first cyclized to the hydantoin and then functionalized with the R^2 substituent with an alkylation reaction, resulting in R^2-substituted intermediates **36a-f**, which were converted in two steps to final compounds using subsequently a Miyaura borylation and Suzuki coupling reaction with intermediates **28a-g**.[27] Reagents and conditions: a) $NaBH_4$, DCM:MeOH (2:1), rt, 80 min, 99%; b) Et_3N, Ms-Cl, THF, 0°C, 45 min, 72%; c) R^1-H, K_2CO_3, ACN, 50°C, 49-95%; d) (4-formyl)boronic acid, $Pd(PPh_3)_4$, K_2CO_3, Toluene:EtOH (4:1, degassed), 50°C, overnight, 60%-quantitative; e) Methylglycinate, $NaBH(OAc)_3$, THF:MeOH (3:1, dry), rt, overnight; f) NaOCN, AcOH, DCM:water (1:1), rt, 0,5-1; g) NaOMe, MeOH, rt, overnight, 9-43% (over three steps); h) NaOH, 2-aminoacetamide.HCl, $NaBH_4$, MeOH:water (5:1), rt, 26 h, 79%; i) CDI, DMAP, ACN, 60°C, 48 h, 48%; j) R^2-halide, K_2CO_3, DMF, 50°C, 77%-quantitative; k) Glycine, NaOH, $NaBH_4$, MeOH:water (5.5:1), rt, 40 h, 90%; l) I) Et_3N, Boc_2O, water, rt, overnight, II) DMF (cat.), $SOCl_2$, DCM, rt, 210 min, III) Cyclopropylamine, DCM, 0°C, overnight, 97%; m) CDI, DMAP, ACN, 60°C, overnight, 94%; n) KOAc, bis(pinacolato)diboron, $Pd(dppf)Cl_2$, DMF, 75°C, overnight; o) $Pd(PPh_3)_4$, K_2CO_3, Toluene:EtOH (4:1, degassed), 75°C, overnight, 9-87%.

Figure 3: Kinetic characterization of LEI101-agonist library. A) Correlation between KRI values and log k_{off} values. Correlation analysis was performed using a two-tailed Pearson correlation analysis

(r = Pearson coefficient). B) Representative competition association curves from [^{3}H]CP55940 alone, or in presence with a long- (**7**) or short residence time (**2**) agonist. C) Kinetic map of log k_{on} vs log k_{off}, where the diagonals represent the 'Kinetic' K_D value ($K_D = k_{off}/k_{on}$). A-C) Data with error is the mean and SEM of three independent experiments performed in duplicate and transformed data without error bars (log k_{on} and log k_{off}) are derived from the mean of three independent experiments performed in duplicate.

Figure 4. Comparison between equilibrium binding affinity and binding kinetics. A-D) Correlation plots of equilibrium affinity (pK_i) with the negative logarithmic transformation of kinetic affinity (pK_D) (A), residence time (RT) (B), dissociation rate k_{off} (C) and association rate k_{on} (D). All data with errors is the mean and SEM of three independent experiments performed in duplicate. Transformed data without error bars (K_D, log k_{on} and log k_{off}) are derived from the mean of three independent experiments performed in duplicate. Correlation analysis was performed using a two-tailed Pearson correlation analysis (r = Pearson coefficient).

Figure 5. Correlation plots of lipophilicity and binding kinetics of group A agonists . A-C) Correlation plot of equilibrium affinity (A), association rate k_{on} (B) or residence time (RT) (C) with cLogP values. Correlation analysis was performed using a two-tailed Pearson correlation analysis (r = Pearson coefficient). All data shown with errors are the mean and SEM of three independent experiments performed in duplicate.

Figure 6. Correlation plots of lipophilicity and binding kinetics of group B agonists. Correlation plot of residence time (RT) and cLogP values. Correlation analysis was performed using a two-tailed Pearson correlation analysis (r = Pearson coefficient). Data shown with errors are the mean and SEM of three independent experiments performed in duplicate.

Figure 7. Correlation plots of residence time and potency of Group A agonists. Correlation plot of potency (pEC_{50}) in G protein activiation (A) or β-Arrestin (B) with residence time (RT). Correlation analysis was performed using a two-tailed Pearson correlation analysis (r = Pearson coefficient). Data shown with errors are the mean and SEM of three independent experiments performed in duplicate.

A

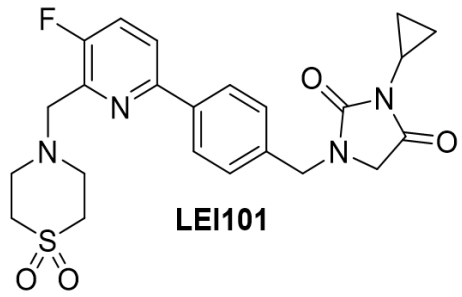

LEI101

B

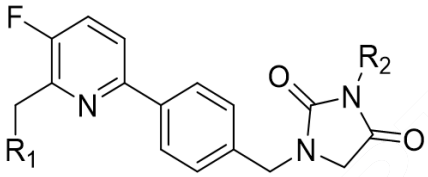

1-28

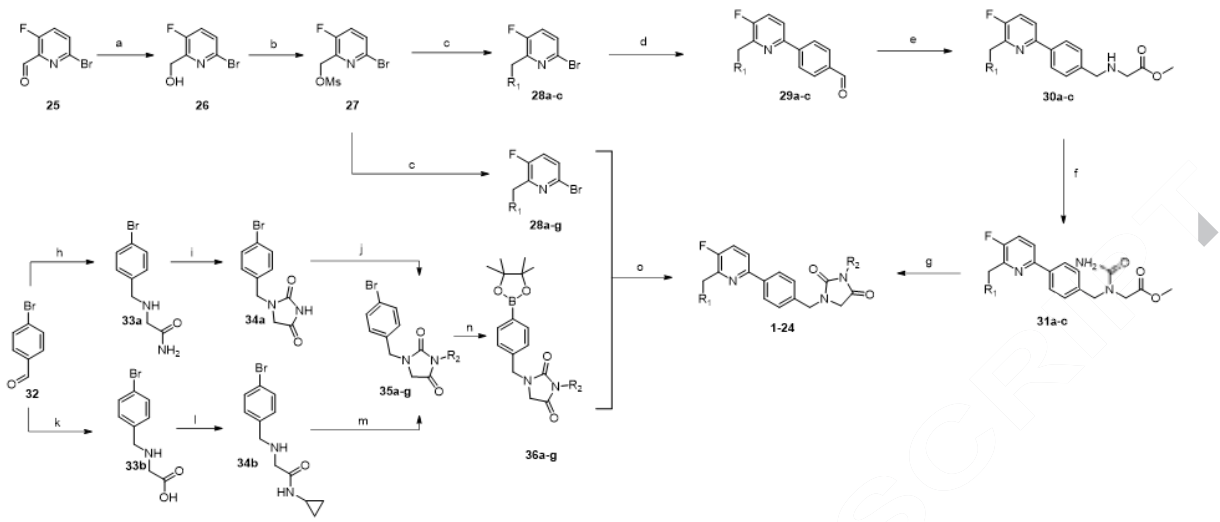

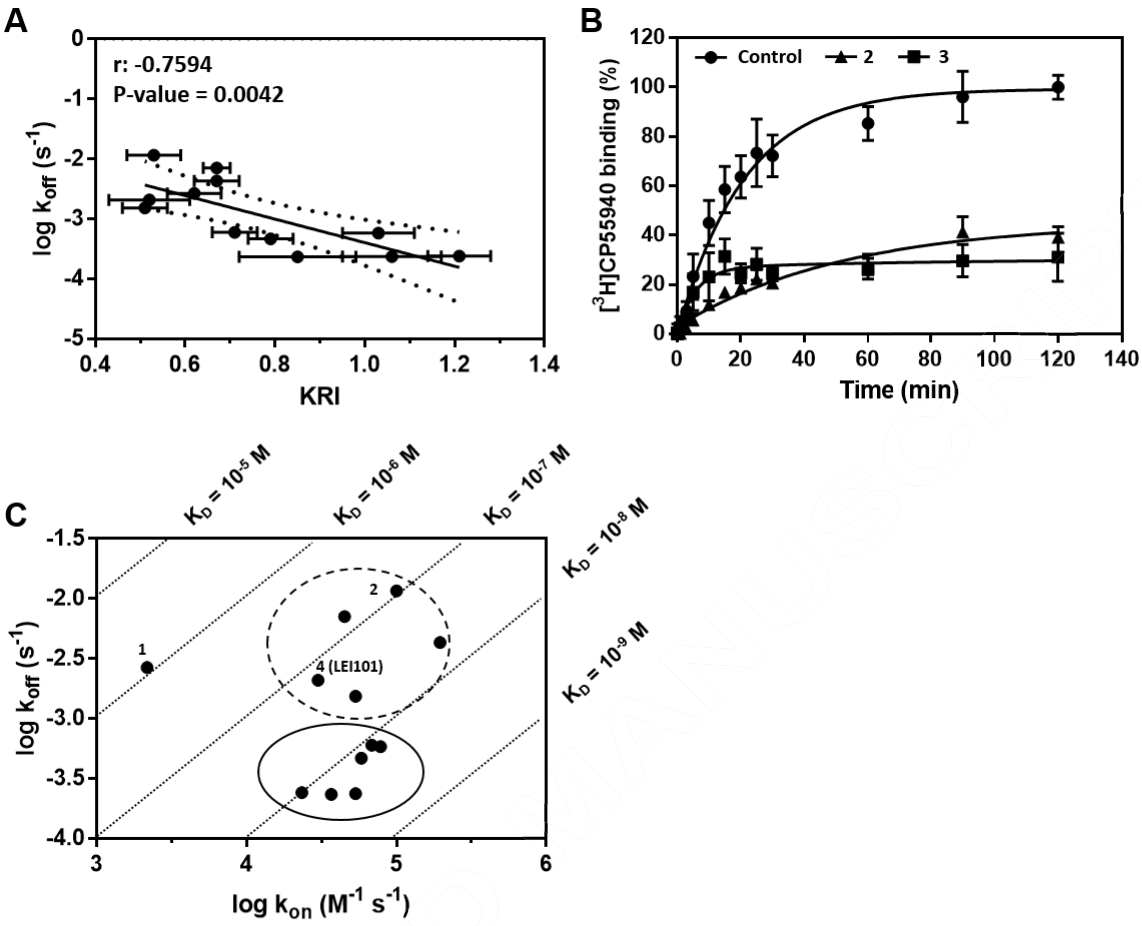

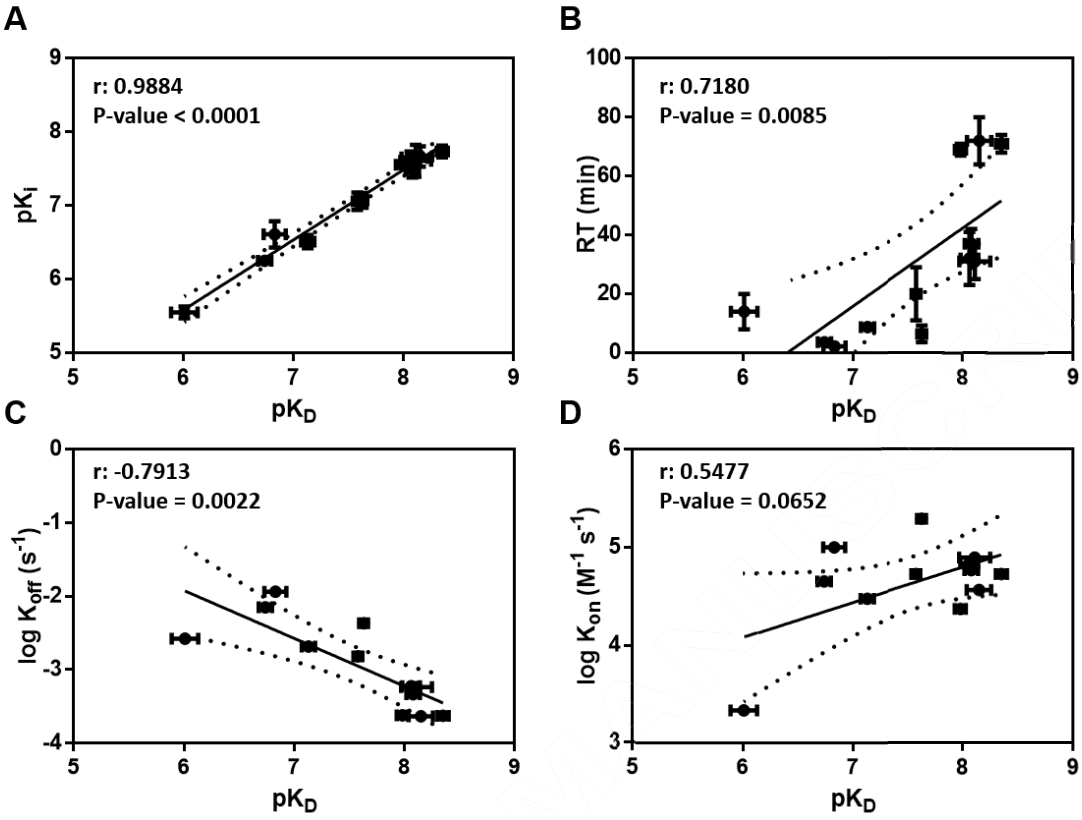

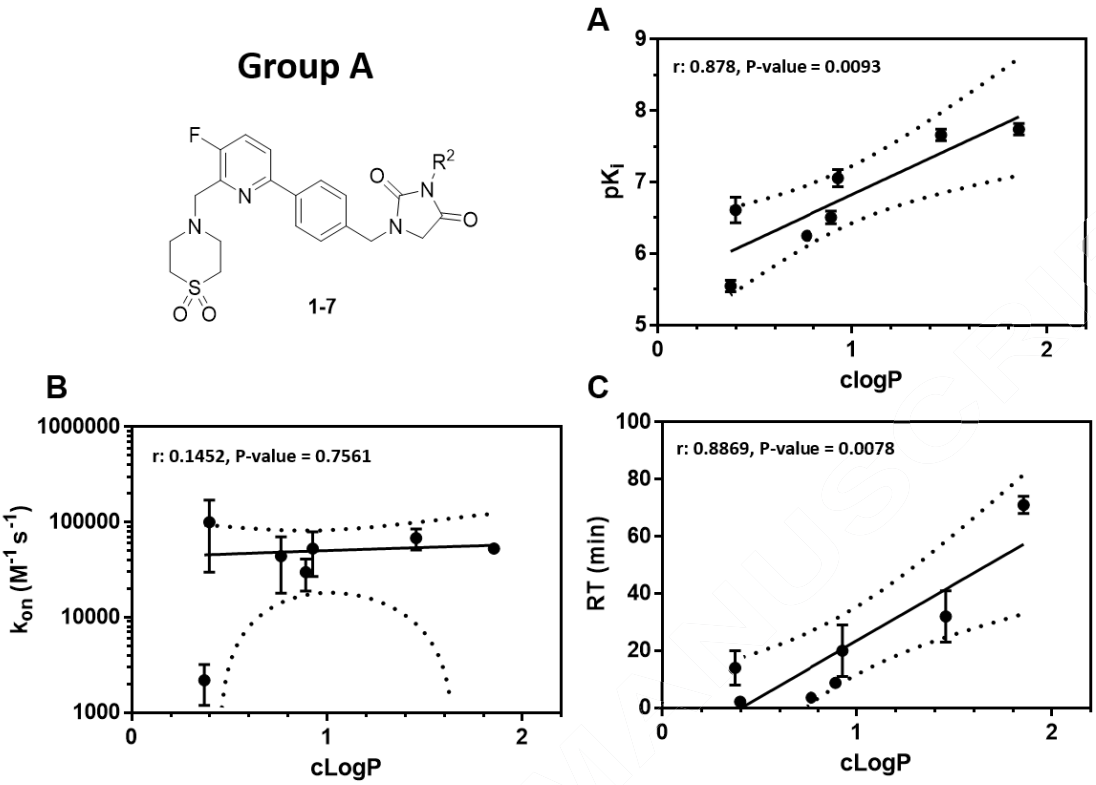

Group B

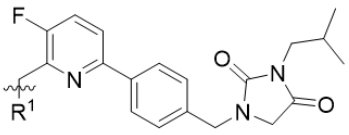

7, 8, 15, 17, 22, 23

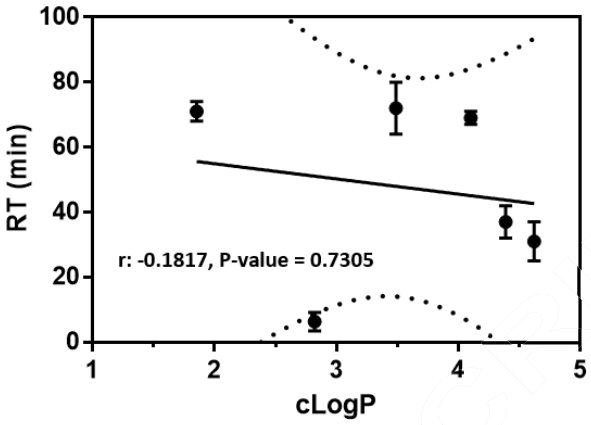

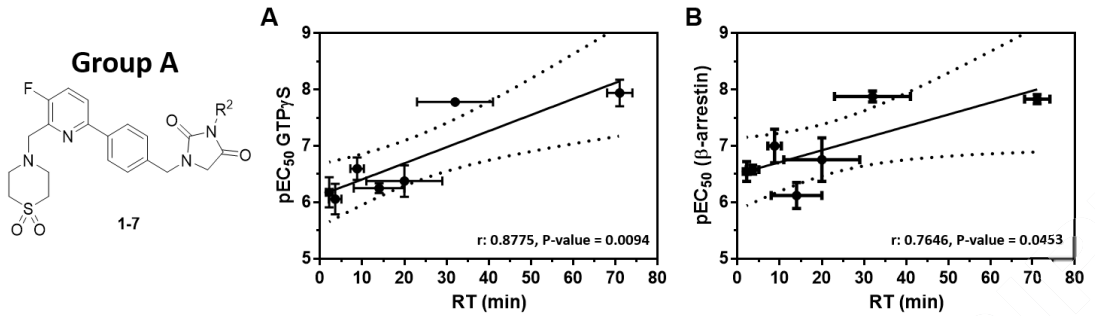

Graphical abstract